USGS
science for a changing world

# High-Resolution Aeromagnetic Survey To Image Shallow Faults, Poncha Springs and Vicinity, Chaffee County, Colorado

By V.J.S. Grauch and Benjamin J. Drenth

**Prepared in cooperation with the Colorado Governor's Energy Office**

Open-File Report 2009-1156

**U.S. Department of the Interior**
**U.S. Geological Survey**

**U.S. Department of the Interior**
KEN SALAZAR, Secretary

**U.S. Geological Survey**
Suzette M. Kimball, Acting Director

U.S. Geological Survey, Reston, Virginia 2009

For product and ordering information:
World Wide Web: http://www.usgs.gov/pubprod
Telephone: 1-888-ASK-USGS

For more information on the USGS—the Federal source for science about the Earth,
its natural and living resources, natural hazards, and the environment:
World Wide Web: http://www.usgs.gov
Telephone: 1-888-ASK-USGS

Suggested citation:
Grauch, V.J.S. and Drenth, B.J., 2009, High-resolution aeromagnetic survey to image shallow faults, Poncha Springs and vicinity, Chaffee County, Colorado : U.S. Geological Survey Open-File Report 2009-1156, 31 p.

# Contents

# Figures

Conversion Factors

| Multiply | By | To obtain |
|---|---|---|
| | Length | |
| meter (m) | 3.281 | foot (ft) |
| kilometer (km) | 0.6214 | mile (mi) |
| meter (m) | 1.094 | yard (yd) |
| | Area | |
| square kilometer ($km^2$) | 247.1 | acre |
| square kilometer ($km^2$) | 0.3861 | square mile ($mi^2$) |
| | Geophysical Parameters | |
| A/m | 0.001 | $emu/cm^3$ |
| magnetic susceptibility (SI) | $1/(4\pi) = 0.079577$ | magnetic susceptibility (cgs) |

Horizontal coordinate information is referenced both to the North American Datum of 1927 (NAD27) and 1983 (NAD83), as noted.

## Abbreviations Used in This Report

| | |
|---|---|
| A/m | amperes per meter |
| cgs | centimeter, gram, second |
| ft | feet |
| km | kilometer, kilometers |
| m | meter, meters |
| mi | mile, miles |
| nT | nanoteslas |
| HGM | horizontal-gradient magnitude |
| RTP | reduced-to-pole |
| SI | Système International |

# High-Resolution Aeromagnetic Survey To Image Shallow Faults, Poncha Springs and Vicinity, Chaffee County, Colorado

By V.J.S. Grauch and Benjamin J. Drenth

## Abstract

High-resolution aeromagnetic data were acquired over the town of Poncha Springs and areas to the northwest to image faults, especially where they are concealed. Because this area has known hot springs, faults or fault intersections at depth can provide pathways for upward migration of geothermal fluids or concentrate fracturing that enhances permeability. Thus, mapping concealed faults provides a focus for follow-up geothermal studies. Fault interpretation was accomplished by synthesizing interpretative maps derived from several different analytical methods, along with preliminary depth estimates. Faults were interpreted along linear aeromagnetic anomalies and breaks in anomaly patterns. Many linear features correspond to topographic features, such as drainages. A few of these are inferred to be fault-related. The interpreted faults show an overall pattern of criss-crossing fault zones, some of which appear to step over where they cross. Faults mapped by geologists suggest similar crossing patterns in exposed rocks along the mountain front. In low-lying areas, interpreted faults show zones of west-northwest-, north-, and northwest-striking faults that cross ~3 km (~2 mi) west-northwest of the town of Poncha Springs. More easterly striking faults extend east from this juncture. The associated

aeromagnetic anomalies are likely caused by magnetic contrasts associated with faulted sediments that are concealed less than 200 m (656 ft) below the valley floor. The faults may involve basement rocks at greater depth as well. A relatively shallow (<300 m or <984 ft), faulted basement block is indicated under basin-fill sediments just north of the hot springs and south of the town of Poncha Springs.

## Introduction

Rift zones are known around the world as geothermally active areas, where deep, hot water is brought to shallow levels via basin-bounding faults (Duffield and Sass, 2003). Understanding the nature of basin faults along which the thermal fluids flow is key to successful exploration for new geothermal resources in these environments. However, basin faults are commonly covered by alluvium, making them difficult to locate and map. Moreover, drill holes, seismic surveys, and other small-scale geophysical surveys cannot give a comprehensive view of fault attitudes and patterns because the information they provide is only for limited areas.

High-resolution aeromagnetic surveys flown over Rio Grande rift basins in northern New Mexico and the active geothermal field in Dixie Valley, Nev., have demonstrated that aeromagnetic methods can successfully map concealed and poorly exposed faults in basin environments (Grauch, 2002; Smith and others, 2002; Grauch and Hudson, 2007). The surveys provide a new view of the overall pattern of faulting and allow general estimates of the attitudes, depths, and geometries of many of the faults.

The Poncha Springs area is at the southern end of the Upper Arkansas Valley, one of the northernmost basins that form the Rio Grande rift. Recent assessments of geothermal potential in Colorado show promise for finding geothermal resources in this area based on high heat flow, presence of hot springs, and complicated zones of faulting (Barret and Pearl, 2006; Berkman and Carroll, 2008).

However, the fault patterns in the area are poorly understood; many of them are concealed and can only be inferred (Van Alstine, 1975; Shannon and McCalpin, 2006).

To better understand the fault pattern in Poncha Springs and vicinity, the Colorado Governor's Energy Office provided funding for the U.S. Geological Survey (USGS) to acquire and process a high-resolution helicopter magnetic survey (fig. 1; Drenth and others, 2009). The Colorado Geological Survey partnered with the USGS to guide the planning of the survey location and goals. This report describes the acquisition and processing procedures for these data, interpretation techniques used to image shallow faults, results of interpretation, and limitations of these results.

## Geophysical Background

Aeromagnetic surveys measure the total intensity of the Earth's magnetic field from an aircraft as it follows a regular pattern of flight lines. The measured magnetic-field data are processed to remove time-varying external fields and are corrected for noise from aircraft movements. The effects of Earth's primary magnetic field are removed to produce "magnetic anomaly data" that isolate subtle variations related to geology. These subtle variations are produced by the distribution of magnetic minerals (normally magnetite) in the ground. The distributions are commonly related to particular rock types. Thus, analyzing the magnetic-field measurements to determine this distribution gives clues to subsurface geology.

For this report, most of the analysis is applied to gridded data and depicted as color shaded-relief images. Individual features on these images are commonly referred to as "anomalies", a term originally developed to describe enclosed areas on contoured magnetic maps. Anomalies are loosely defined by areas that contain increasing values that culminate in relative maxima (a "high") or decreasing values

that culminate in relative minima (a "low"). The range of values of an anomaly define its "amplitude"

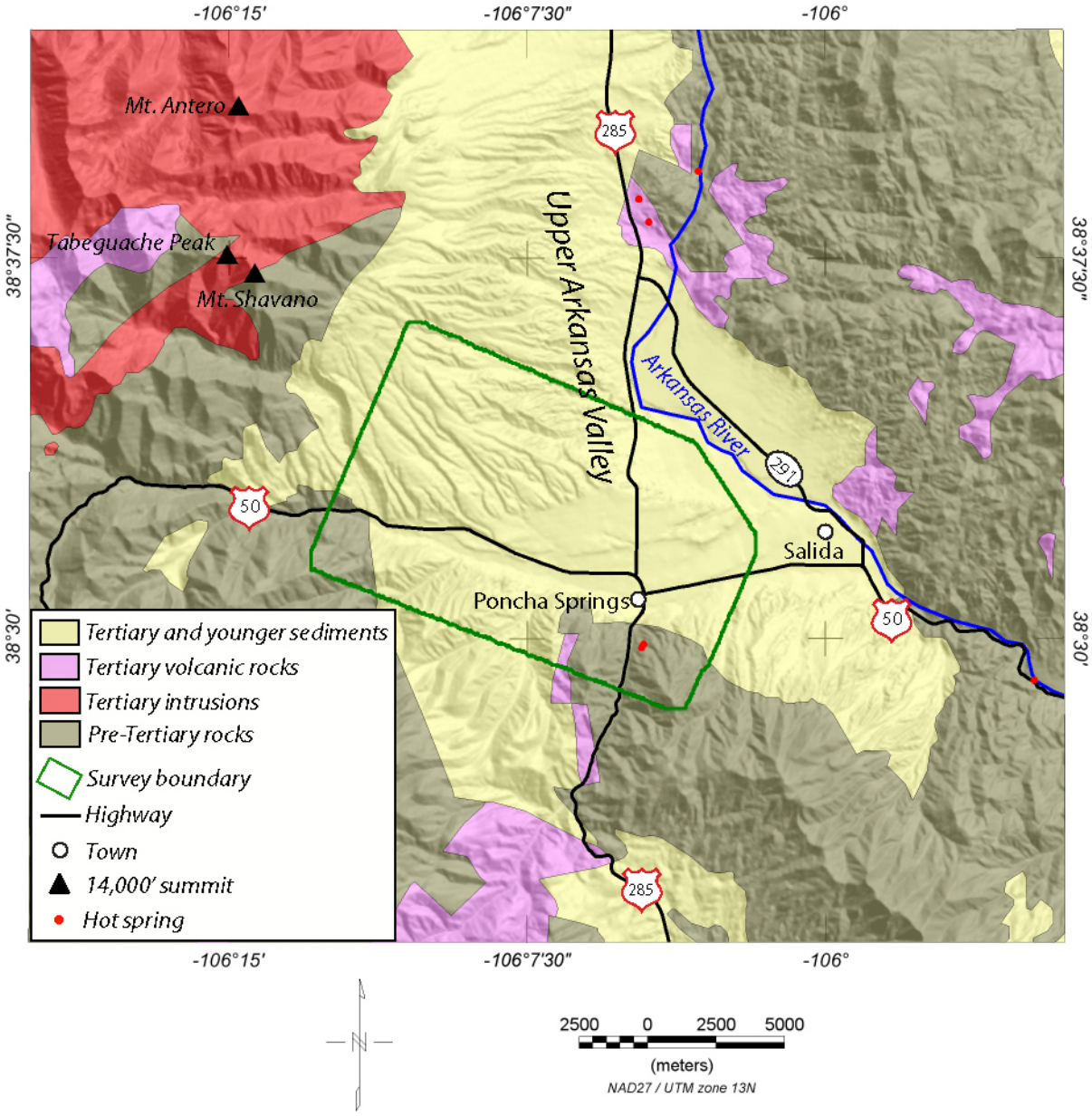


**Figure 1.** Physiography and simplified geology (Tweto, 1979) of the region around Poncha Springs, Colorado.

(always a positive number), and the areas of steep decrease or increase (sides of the anomaly) are anomaly "gradients."

Magnetic properties of rocks and sediments are determined by the quantity of magnetic minerals, their mode and age of their formation, and their thermal and geochemical history. The quantity of magnetic minerals appears to be the primary variable determining magnetic-field variations in this study area (Case and Sikora, 1984), measured as "magnetic susceptibility" (a dimensionless quantity dependent on the system of measurement; see list of conversion factors). Magnetic susceptibility is multiplied by the Earth's magnetic field intensity (using proper unit conversions; Hansen and others, 2005) to represent the "magnetization" of a particular geologic unit in magnetic models. Magnetization is reported in amperes/meter (A/m) in Système International (SI) units. Mafic and ultramafic igneous and metamorphic rocks typically contain the greatest abundance of magnetic minerals (high magnetic susceptibilities), and sedimentary rocks and sediments typically contain the least abundance (Reynolds and others, 1990). Anomalies related to faults, the focus of this report, are produced by a significant contrast in magnetic properties of rocks or sediments that are juxtaposed at a fault.

## Survey Design

Conventional aeromagnetic surveys are designed to focus on mapping magnetic rocks, such as igneous and metamorphic basement rocks. High-resolution surveys are flown closer to the ground and with narrower line spacing. This survey design allows better detection of subtle magnetic contrasts, such as those arising from the juxtaposition of basin-fill sediments having different lithologies. It also allows for better definition of sources with limited lateral extent and for better overall resolution of details in map view.

Design of the Poncha Springs survey was guided by the high-resolution surveys that were successful for the basins of the northern Rio Grande rift in New Mexico. These surveys were flown with fixed-wing airplanes and helicopters along traverse lines spaced 150–200 m (~500–660 ft) apart and 150 m (~500 ft) above the ground.

The large amount of topographic relief in the Poncha Springs region dictated the use of a helicopter for the survey. Helicopter systems allow low magnetometer heights because helicopters can follow the terrain more closely than fixed-wing aircraft. A low magnetometer height improves detection of subtle magnetic contrasts, but the increased cost of flying a helicopter encourages wider line spacing to cut down on the total miles flown. These considerations also must take into account safety considerations and the need for proper sampling; a ratio between 1:1 and 2:1 of line spacing to height above magnetic sources is considered adequate in order to sample sources between lines (Reid, 1980). Optimum specifications for the Poncha Springs survey required traverse lines flown generally northeast-southwest (oblique to the dominant strike of geologic units) spaced 150 m (~500 ft) apart, a magnetometer height of 150 m above ground, and tie lines oriented northwest-southeast and spaced 1.5 km (~5000 ft) apart. Tie lines are commonly used to "level" the traverse lines and minimize errors inherent in normal flight operations. Survey specifications are summarized as follows:

1. ***Dates of Acquisition***: October 25—October 29, 2008
2. ***Line Spacing***: 150 m (~500 ft), lines trend N23ºE—perpendicular to regional structures
3. ***Tie Lines***: 1500 m (~5000 ft), lines trend N67ºW—parallel to regional structures
4. ***Observation Height Above Ground***: 150 m (~500 ft), minimum height given safety considerations
5. ***Instrument/Aircraft***: Cesium-vapor magnetometer with sampling rate of 0.1 seconds mounted in a stinger assembly on a Bell 206 B3 helicopter
6. ***Area Surveyed***: ~138 $km^2$ (~53 $mi^2$)
7. ***Total Flight-Line Length***: 963 line km (598 mi)

The high resolution gained by this survey design provides a good definition of anomalies related to shallow sources, which are associated with local gradients (gradients with limited lateral extent). The

local gradients can then be separated from the broader gradients of the deeper sources, even those that produce anomalies with much higher amplitudes. The separation comes during the interpretation phase of the project, discussed below.

## Data Acquisition and Processing

Under contract to the USGS, New Sense Geophysics Limited of Toronto, Ontario, Canada, and Upper Limit Aviation Inc. (ULA) of Salt Lake City, Utah, undertook the acquisition and processing of a helicopter-borne magnetic survey during the period October 25 through October 29, 2008. The survey area covers part of the Upper Arkansas Valley, Chaffee County, in central Colorado, and focuses on the southwestern portion of the valley and geothermal springs near the town of Poncha Springs (fig. 1). Eight flights were needed to complete the acquisition of 963 line kilometers (598 mi) of airborne data. Weather and geomagnetic conditions were generally favorable during the fieldwork. Final data processing was completed by the end of January 2009. The final, processed, total-field magnetic flight line data were gridded using a minimum-curvature routine with a grid spacing of 50 meters (one third of the line spacing of the survey) and draped at a constant distance of 100 m (~300 ft) above the ground using analytical continuation. Data acquisition, processing procedures, and digital data from the survey are described in greater detail in Drenth and others (2009).

## Methods of Analysis

Several interpretation methods were applied with the goal of enhancing the signature of shallow faults and estimating the depths to the magnetic contrasts along the faults. The methods included reduction-to-pole, gradient window, analysis of terrain effects, first vertical derivative, and depth estimation using the local wavenumber method. These techniques are useful for mapping the locations of steeply dipping magnetic contrasts but may not be as useful for detecting magnetic contrasts with

shallow dips. One anomaly likely related to pre-Tertiary bedrock and possibly to a shallowly dipping magnetic contrast near known hot springs was examined in further detail.

### Reduction-to-Pole

A reduction-to-pole (RTP) transformation is commonly applied to aeromagnetic data to minimize polarity effects (Baranov and Naudy, 1964; Blakely, 1995). Polarity effects are manifested as a shift of the main anomaly away from the center of the magnetic source and are due to the vector nature of the measured magnetic field. This procedure greatly facilitates inspection of aeromagnetic maps and their comparison to geology. The RTP transformation usually involves an assumption that the total magnetizations of most rocks align parallel or anti-parallel to the Earth's main field (declination = 10º, inclination = 65º for the study area). This assumption probably works well for most of the Tertiary and younger units in the study area and appears to be applicable for older rocks in the region as well (Case and Sikora, 1984). The RTP aeromagnetic data, computed from a grid of the total-field magnetic data, are displayed in figures 2 and 3 as color shaded-relief maps with different illumination directions.

### Gradient Window Method

The RTP magnetic data reveal subtle linear anomalies (<10 nT) superposed on the larger magnetic anomalies (figs. 2 and 3). To enhance the signature of these faults, the gradient window method was applied (Grauch and Johnston, 2002), which is a modification of the horizontal-gradient method (Cordell and Grauch, 1985; Blakely and Simpson, 1986). The horizontal-gradient method is based on a principle from gravity methods that steep gradients occur over near-vertical contacts between units with differing physical properties. For magnetic data, the same principle can be applied to the RTP data, although care must be taken to avoid interpreting spurious lineaments that may result (Grauch

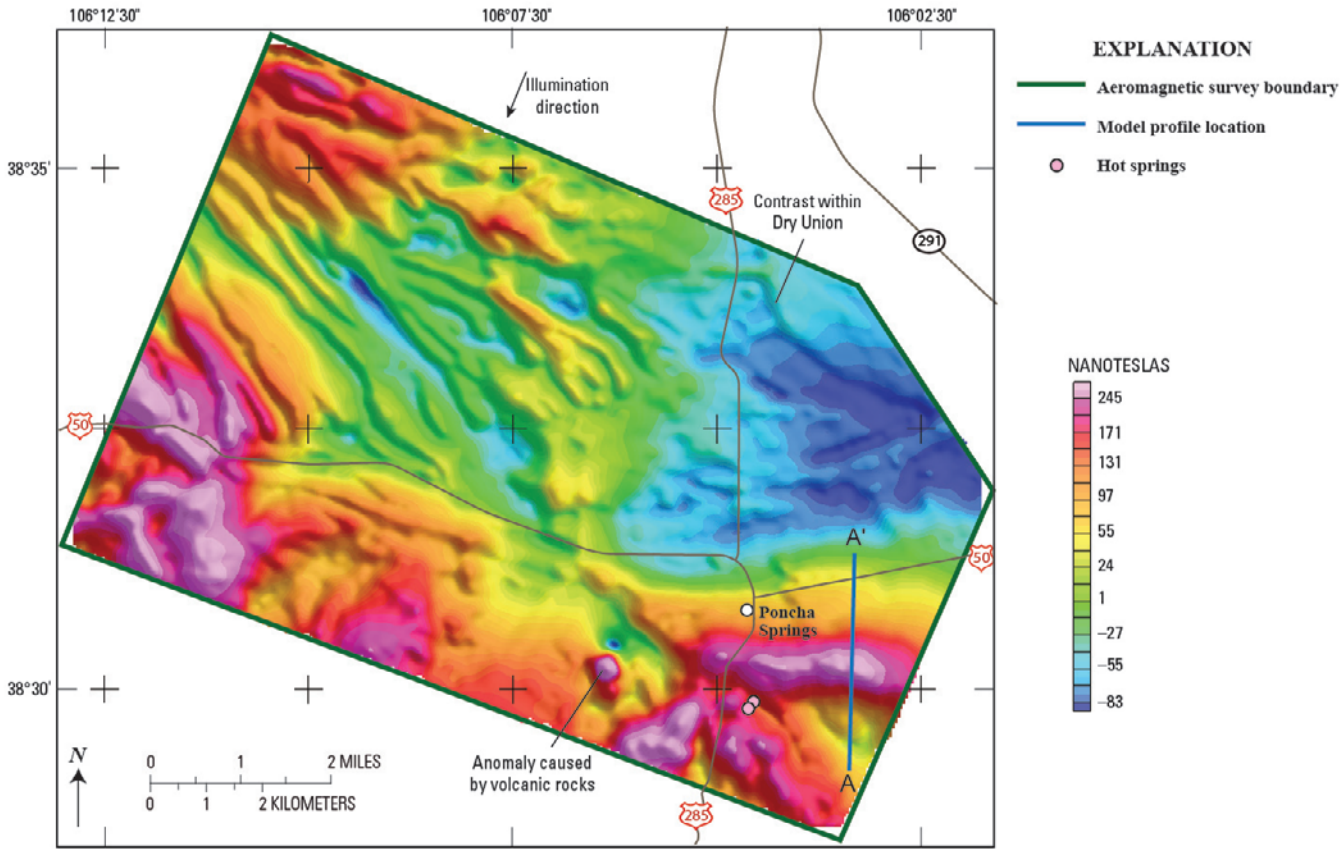


**Figure 2.** Reduced-to-pole (RTP) aeromagnetic data shown in color shaded-relief, illuminated from the northeast. The colors best display the broad variations in the magnitude of magnetic data, whereas the shading highlights gradients, especially those that are linear. The northeast illumination enhances northwest lineaments.

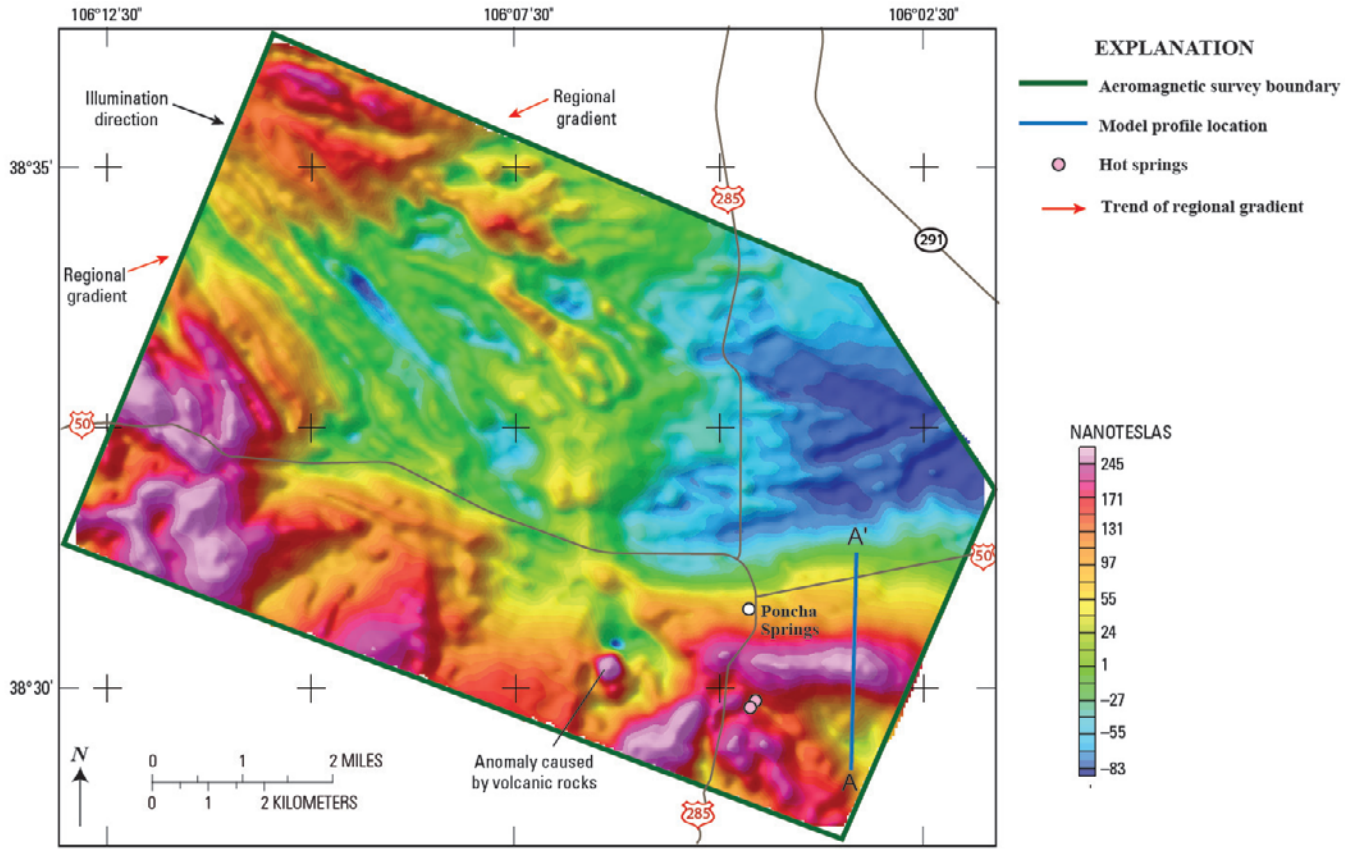


**Figure 3.** Reduced-to-pole (RTP) aeromagnetic data shown in color shaded-relief, illuminated from the northwest. The colors best display the broad variations in the magnitude of the magnetic data, whereas the shading highlights gradients, especially those that are linear. The northwest illumination enhances north-south lineaments.

and others, 2001; Grauch and Hudson, 2007). Local peaks (or ridges) in the magnitude of the horizontal gradient of the RTP data give the locations of the steepest gradients, intuitively similar to taking the first derivative of a curve. The gradient window method isolates the horizontal-gradient magnitudes (HGM) associated with the short-wavelength anomalies (Grauch and Johnston, 2002) in order to focus on locating shallow, near-vertical contacts. The HGM map resulting from gradient window application to the Poncha Springs RTP data is shown in figure 4.

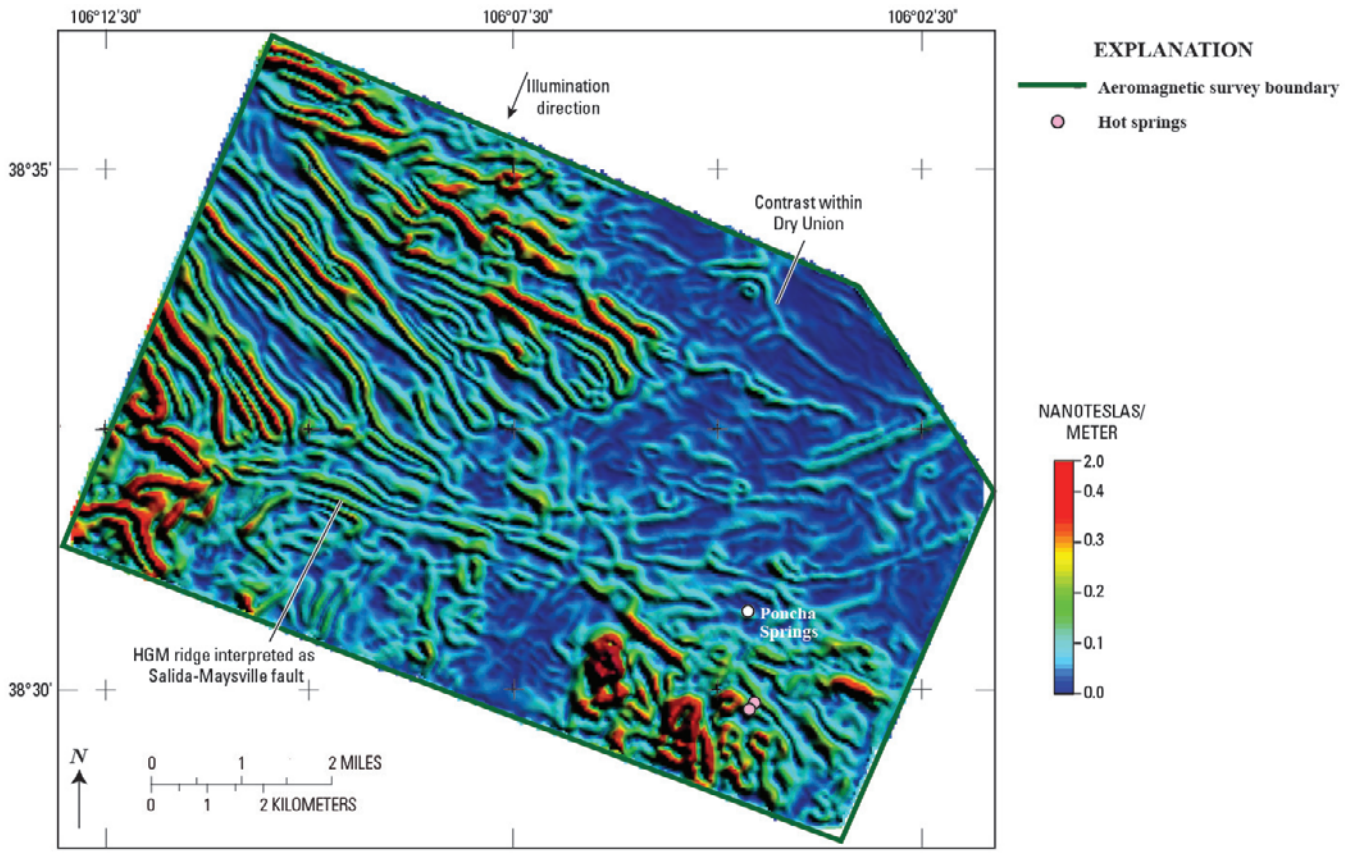


**Figure 4.** Color shaded-relief image of the HGM associated with local (shallow) features, computed from the RTP data using the residual after removing a plane from a 1.25 x 1.25 km moving window using the gradient window method. Illuminated from the northeast.

## Analysis of Terrain Effects

Terrain that is strongly magnetized produces magnetic anomalies that mimic the shape of the terrain. Several linear magnetic anomalies in the northwestern portion of the survey follow the trends of the topography (compare figs. 2 or 3 with 5). Such linear features do not necessarily indicate the locations of lithologic contrasts or faults, because they can be explained by the surface topography alone. On the other hand, faults and geologic contacts commonly produce topographic scarps, so their

correspondence to aeromagnetic anomalies may require field-checking to determine if the source is solely topographic.

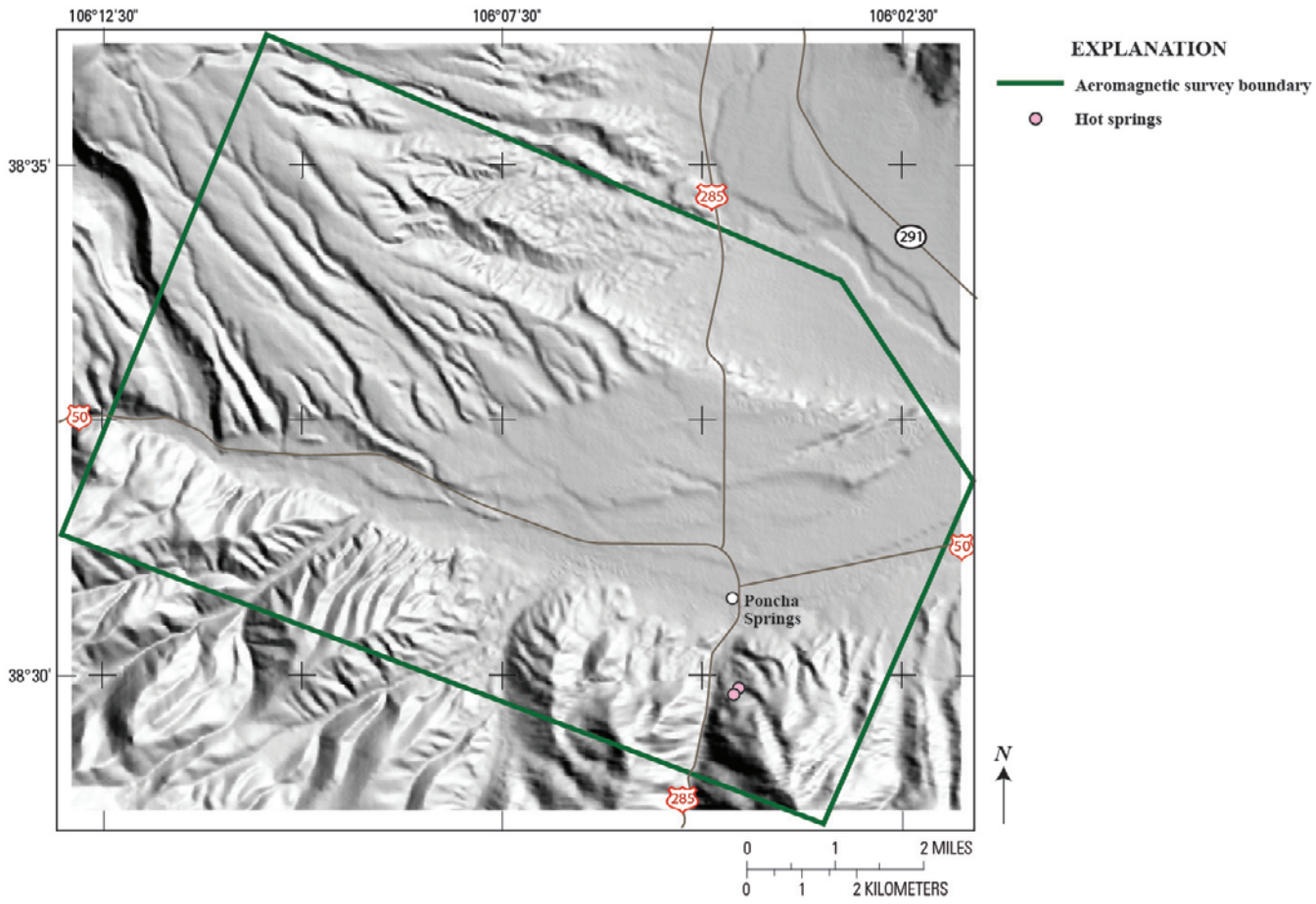


**Figure 5.** Gray shaded-relief image of terrain within the Poncha Springs region. Topographic relief within the survey area is 914 m (3,000 ft). Elevation of Poncha Springs is 2,275 m (7,465 ft).

To identify the role of terrain in causing aeromagnetic anomalies, we used (1) a qualitative comparison of terrain (fig. 5) versus aeromagnetic maps, and (2) a quantitative comparison of the shapes and magnitudes of simulated magnetic fields (assuming uniformly magnetized terrain) versus the observed aeromagnetic data. For the quantitative comparison, we computed the magnetic effect of uniformly magnetized terrain using a modeling method that uses a vertical prism below each grid point of a digital elevation model (prism algorithm of Blakely, 1995, implemented by unpublished software of J. Phillips,

USGS). A constant magnetization of 0.42 A/m was chosen for all prisms, which represents a uniform magnetic susceptibility of about 0.010 SI (with the magnitude of Earth's field assumed to be 53,000 nT). This magnetic susceptibility fits with reconnaissance magnetic-susceptibility measurements of alluvium in the area of Poncha Springs and represents the high end of the expected range of values for equivalent basin-fill sediments typical for the northern Albuquerque basin (Hudson and others, 2008). The computed magnetic terrain effects provide a guide to the shapes of anomalies that would occur if magnetic anomalies were produced solely from magnetic material underlying the ground surface. Using this simulation, the HGM of both observed (fig. 4) and simulated (fig. 6) anomalies can be directly compared. Figure 7 shows the results of analysis of the HGM comparison for the survey area.

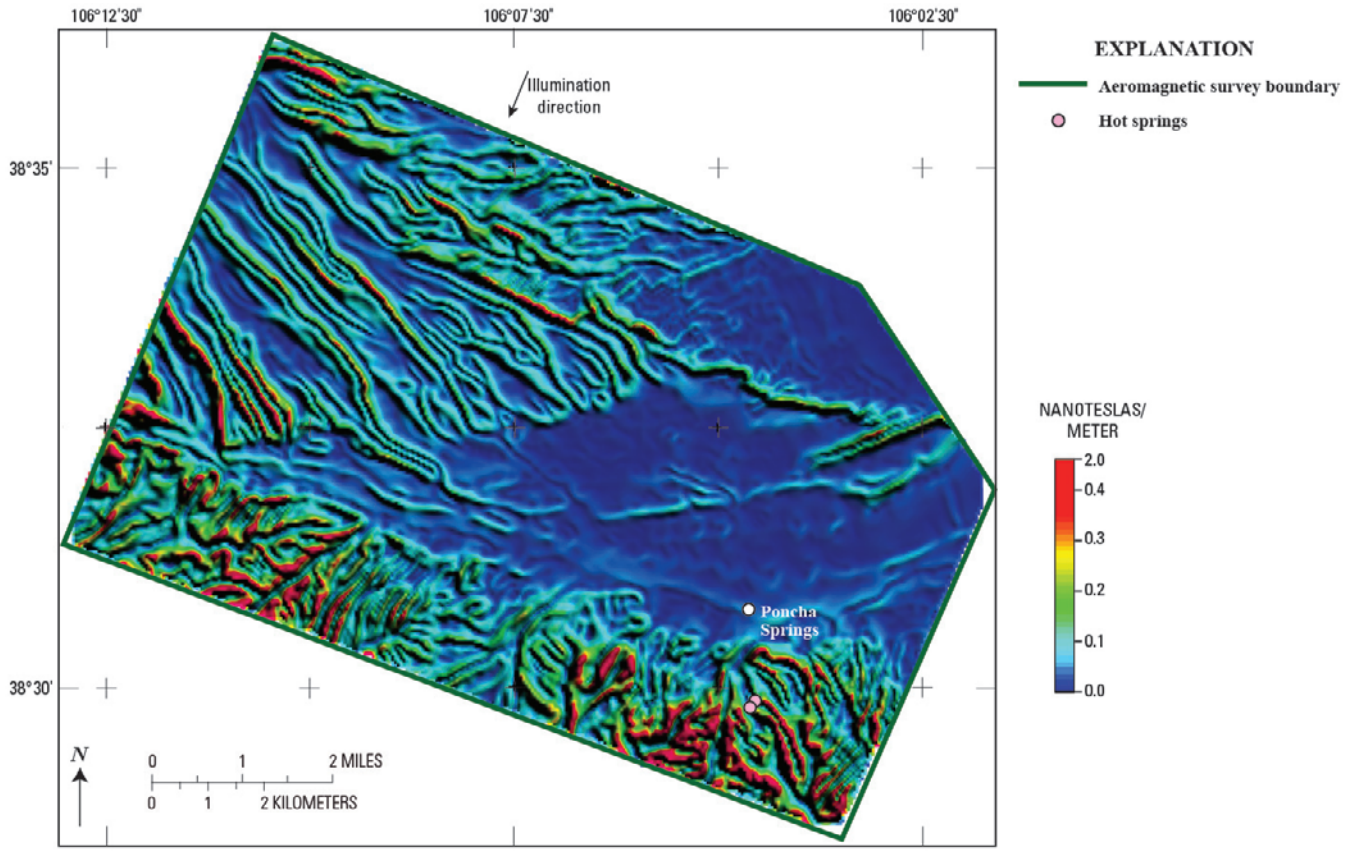


**Figure 6.** Color shaded-relief image of the HGM of simulated magnetic field of terrain for comparison with the HGM of the RTP data (fig. 4). Illuminated from the northeast.

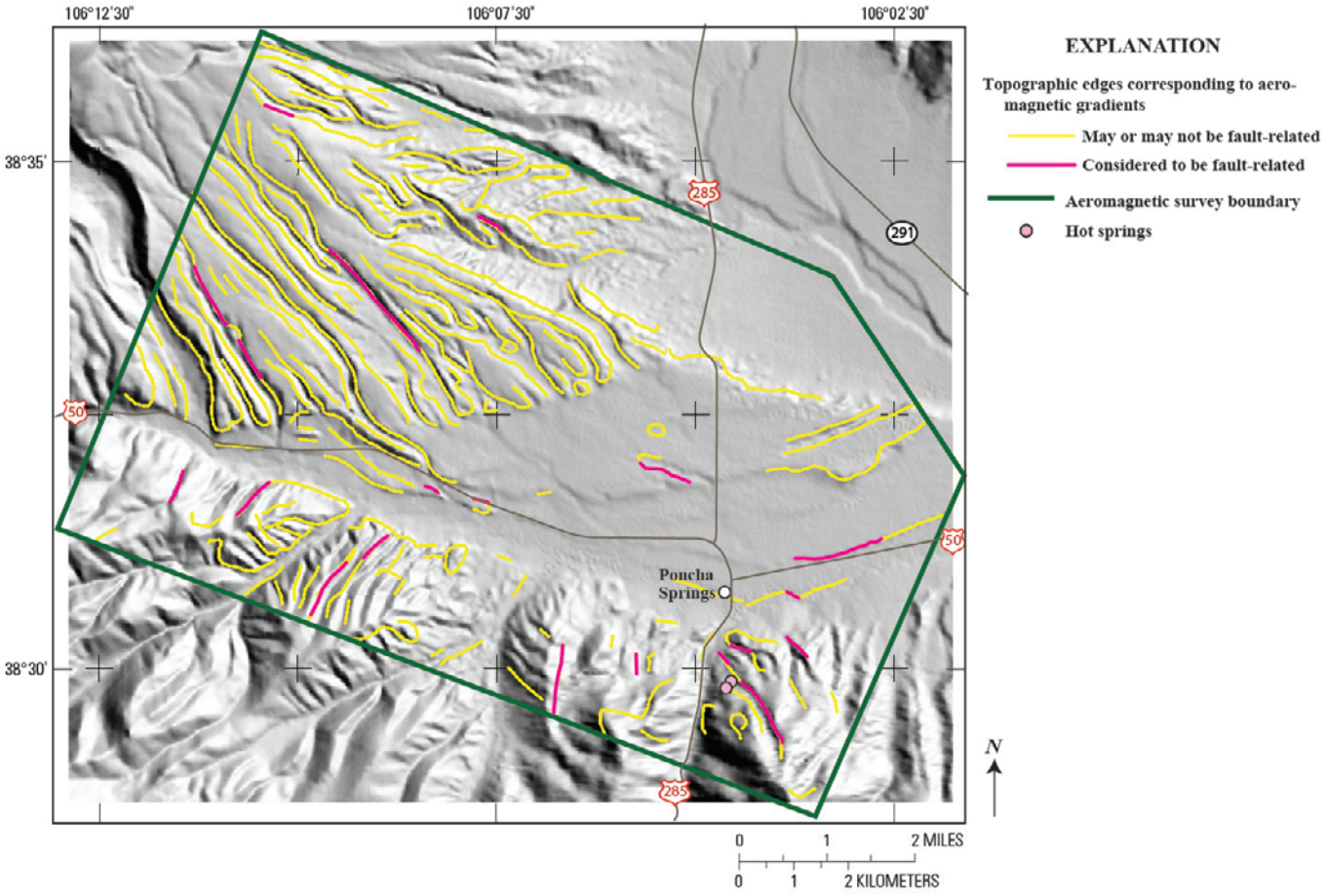


**Figure 7.** Topographic edges corresponding to aeromagnetic gradients and those interpreted as faults. Base is terrain data from figure 5. The correlations were derived by analyzing HGM data derived from both the RTP data and simulated magnetic terrain effects.

## First Vertical Derivative

Another method used to enhance the magnetic signature of near-surface geologic features is a first vertical derivative transformation. This method uses the principle that anomalies related to deeper sources attenuate more slowly than those related to shallow sources. The result is a map (fig. 8) that is a better representation of near-surface features (such as faults) than the original data (figs. 2 and 3). Prominent lineaments on this map may be related to faults that do not produce simple HGM anomalies,

as may be the case for structures that cross several different types of lithologies and terrain. These lineaments are interpreted in a more subjective manner than those detected with the HGM analysis.

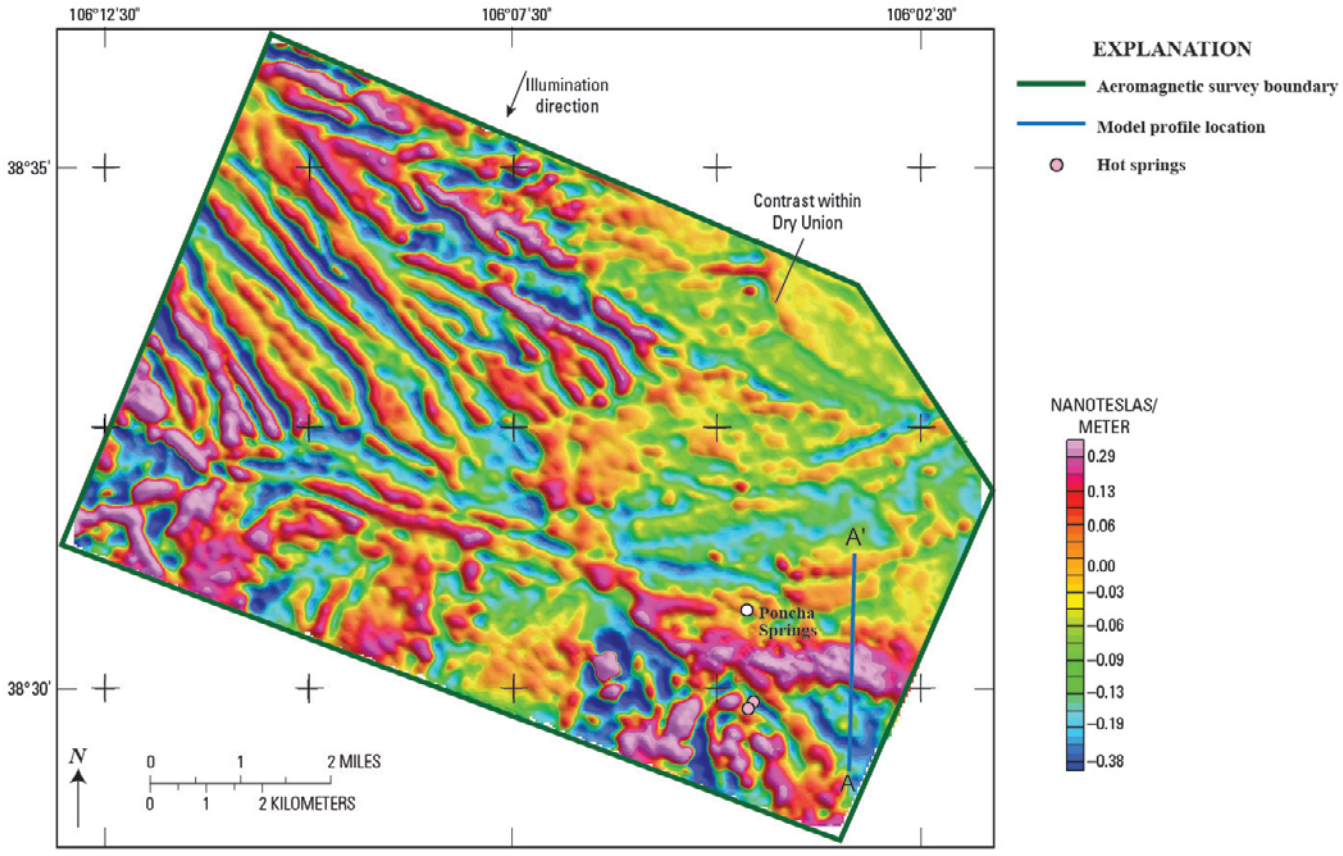


**Figure 8.** First vertical derivative of the RTP data, shown in color shaded-relief and illuminated from the northeast.

## Preliminary Depth Estimation

A depth analysis of the aeromagnetic data is beyond the scope of this report. However, to aid interpretation of individual features, preliminary depth estimation was performed (not shown). We used the local wavenumber method (Thurston and Smith, 1997; Smith and others, 1998; Phillips, 2000; Phillips and others, 2007) for depth estimation because it is an objective method that works well for high-resolution aeromagnetic datasets (such as the Poncha Springs survey). The method relates spatial gradients of the measured magnetic field to the depths of sources, based on the general principle that

shallow sources produce anomalies with steep gradients, whereas deep sources produce anomalies with broad gradients. Because the local wavenumber method is sensitive to noise in the aeromagnetic data, we applied the method to the first vertical integral of the RTP magnetic data, following Phillips and others (2007).

Depths that correspond to interpreted faults are estimated almost entirely to be <200 m (656 ft). The majority of them are in the range of 30–100 m (~100–330 ft). These estimates are reflective of the depths to the magnetic contrasts that cause the aeromagnetic anomalies and therefore not necessarily the depths to the tops of faults.

## Interpretations

Much insight into the sources of the aeromagnetic anomalies comes from initial comparisons to terrain. As discussed previously, terrain-related anomalies provide information about magnetic sources at the surface that can be compared directly to geologic mapping. Inspection of the two displays of the RTP map (figs. 2 and 3) in comparison to terrain shapes (fig. 5) shows good correspondence over the strongly dissected terrain in the northwestern part of the survey area, poor correspondence over the mountainous terrain south of Highway 50, and mixed correspondence elsewhere. The area of good correspondence is also evident by the numerous aeromagnetically expressed topographic edges in the northwest part of the study area (fig. 7). This area is mapped as glacial outwash of multiple ages overlying older rift-fill sediments of the Dry Union Formation (Shannon and McCalpin, 2006). Because access is difficult in this area, further analysis of these anomalies (beyond the scope of this report) may help delineate different mineralogies related to the glacial outwash units.

The area of poor correspondence between anomalies and terrain occurs over mountainous areas along the southern part of the survey area that is mapped as Tertiary sediments (primarily Dry Union Formation) and pre-Tertiary (mainly Precambrian) rocks (fig. 1; Tweto, 1979). The poor

correspondence suggests that the magnetic sources producing the anomalies represent volumes of rocks that are mostly buried. An exception is the prominent circular aeromagnetic high about 0.5 km (0.3 mi) in diameter located about 2.5 km (1.6 mi) west of the hot springs (figs. 2 and 3). This anomaly corresponds to Tertiary volcanic rocks exposed at the surface (fig. 1) that may be broken into segments by faulting (Scott and others, 1975).

The area of mixed correspondence occurs over most of the low-lying terrain in the survey area. The anomalies corresponding to terrain shapes in this area indicate that the valley materials are magnetic enough to produce anomalies and can be verified by field checking. The anomalies that do not correspond to topographic shapes are indicative of magnetic sources that are concealed below the valley floor.

### Faults and Linear Geologic Contacts

The interpretive maps resulting from application of the methods described above were used together to locate possible faults or other linear geologic contacts that juxtapose rocks or sediments of contrasting magnetic properties. These faults or contacts are represented as lines on figure 9. Where these faults or contacts are buried, the lines represent surface projections from the shallowest occurrence of the magnetic contrast across the fault or contact. Whether or not a given magnetic contrast will cause an aeromagnetic anomaly mainly depends on three unknowns: the magnitude of the magnetization contrast between juxtaposed units, the vertical extent of the juxtaposition of the contrasting units, and the depth to the top of the contrast (Grauch and Hudson, 2007). Even faults that juxtapose sediments against sediments, which are typically orders of magnitude lower in magnetization than other rock types, are capable of producing anomalies in the Poncha Springs aeromagnetic survey.

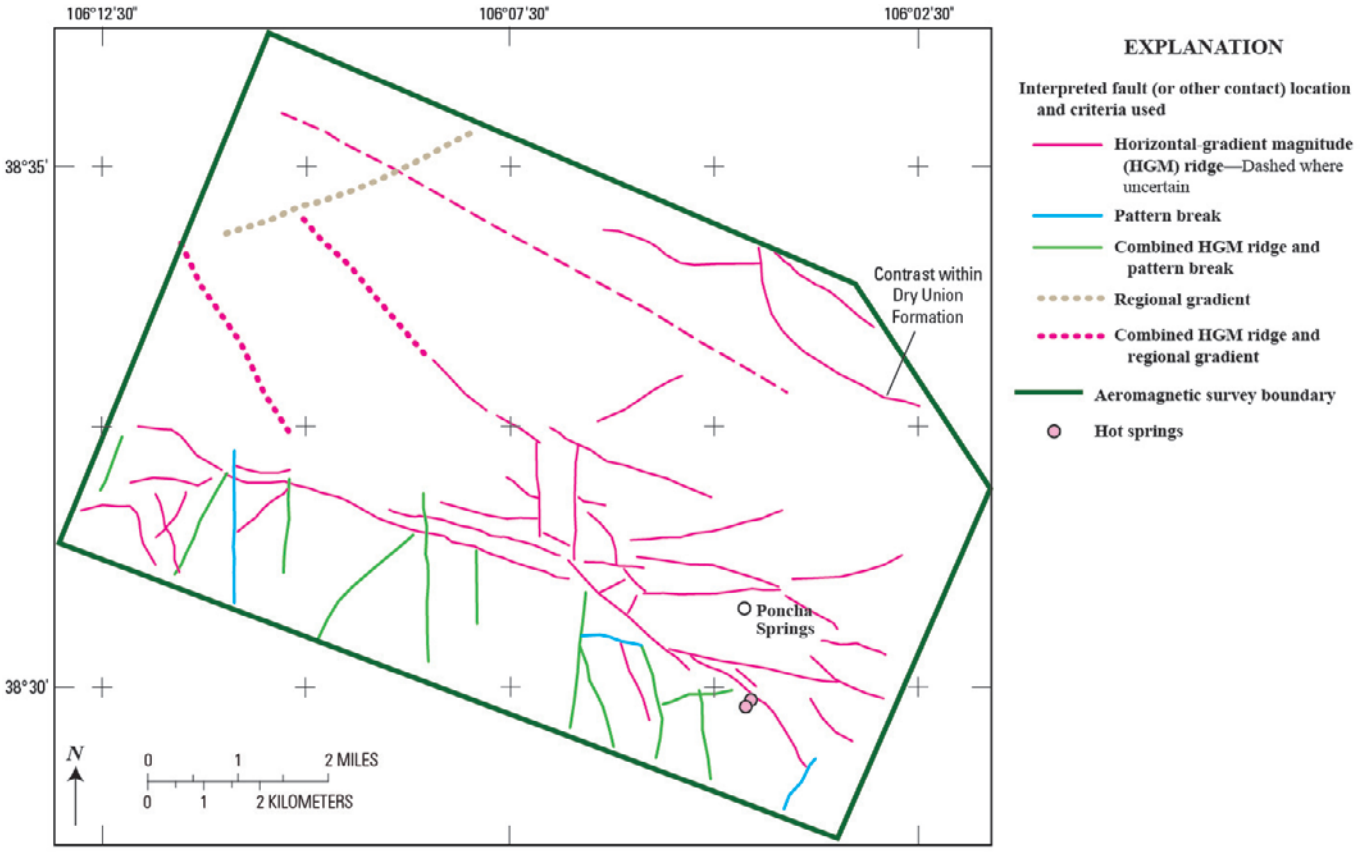


**Figure 9.** Interpreted lines inferred as faults or other linear geologic contacts and criteria used for interpretation.

We followed somewhat different interpretation strategies for each of the three areas having different degrees of correlation between anomalies and terrain. For all areas, lines were drawn using ridges on the HGM map (using criteria suggested by Grauch and Hudson, 2007), at abrupt breaks in patterns in the RTP or first-vertical derivative maps, or along regional gradients (fig. 9). Lines were drawn and interpolated over areas where we judged that different gradient trends were crossing or otherwise interfering with each other. Where HGM ridges correspond to analogous ridges in the simulated magnetic effects of terrain (figs. 4, 6, and 7), faults were interpreted only where terrain analysis, depth estimation, or inspection of other relations provided confident evidence that a magnetic source lies at depth below the topography.

In the area of good correspondence between anomalies and terrain, the aeromagnetic anomalies exhibit more linearity in the patterns than is evident from the terrain map. This difference is demonstrated by comparing the two HGM maps (figs. 4 and 6) or the terrain map (fig. 5) to the first vertical derivative map (fig. 8), which focuses on anomalies caused by shallow sources. The strong northwest linearity of anomalies suggests that the drainage pattern has an underlying structural origin, although geologists generally have mapped faults oblique to this orientation (fig. 10). We tentatively interpret two faults along the northwesterly trends (bold dotted lines on fig. 9) on the basis of regional gradients (broad differences in magnetic data values) that correspond to HGM ridges. These lines both coincide with drainages underlain by alluvium and Dry Union Formation (Shannon and McAlpin, 2006), suggesting that the magnetic sources lie within the Dry Union Formation. A more northeasterly striking fault is interpreted where a regional gradient marks a change from high values on the northwest from low values on the southeast, evident in the RTP map ("Regional gradient" on fig. 3; dotted gray line on fig. 9). The absence of the regional gradient in the first vertical derivative map (fig. 8) implies it is not shallow and that it originates from a magnetic contrast with considerable depth extent, such as a major fault within the Dry Union Formation or a linear contact in underlying basement rocks.

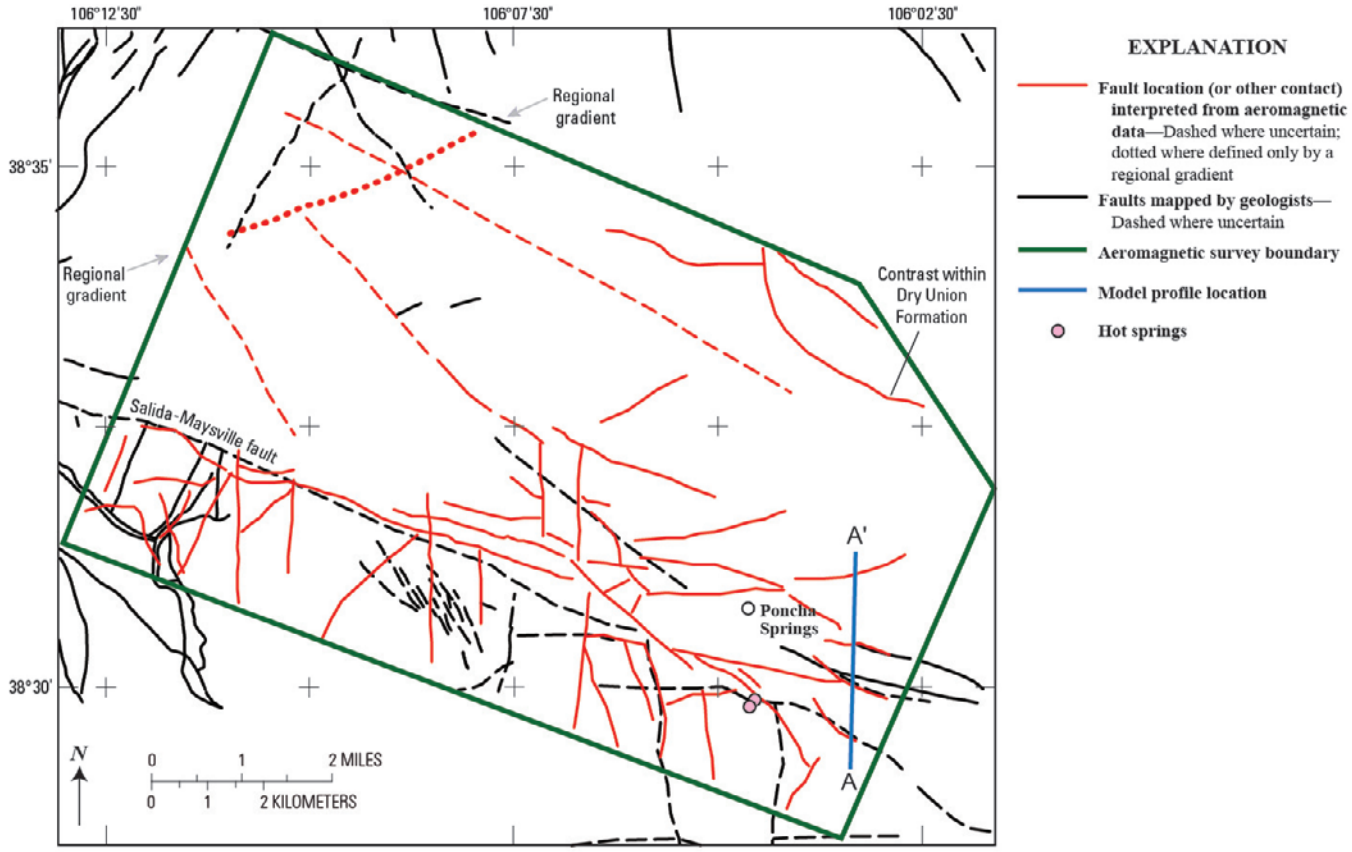


**Figure 10.** Summary of fault interpretations with faults mapped by geologists (from Scott and others, 1975; Van Alstine, 1975; Shannon and McCalpin, 2006). Lineaments of Scott and others (1975) are not included because they were not field checked.

In the mountainous areas south of Highway 50, faults (or other linear contacts) were interpreted both from linear HGM ridges and from abrupt differences in patterns in the RTP or first vertical derivative maps (fig. 9). The major breaks in patterns likely represent major contacts or faults that juxtapose large volumes of differing rock types at depth. Several of these pattern breaks occur in the vicinity of the hot springs, which are manifested in different ways on the RTP, HGM, and first vertical derivative maps (figs. 2, 3, 4, and 8). Lines representing these pattern breaks as well as lines along linear features

indicate faults or linear geologic contacts of multiple orientations in the vicinity of the hot springs (fig. 9).

In the low-lying areas, many linear features are apparent in the RTP maps (figs. 2 and 3) and accentuated in the HGM map (fig. 4). Based on the subtle magnitudes and narrow HGM ridges, most of these appear to arise from contrasts within sediments. Lines were drawn along the HGM ridges to represent faults (fig. 9) where (1) HGM ridges do not correspond to topographic features or (2) HGM ridges that do correspond to topographic features have significantly greater magnitudes than could be caused by a reasonable maximum magnetization for the valley sediments (compared to the simulated magnetic terrain model). In a few cases, multiple HGM ridges closely parallel each other, such as at the Salida-Maysville fault (compare figs. 4 and 10). Multiple HGM ridges commonly occur where the geometry of the juxtaposed layers at the fault results in magnetic contrasts that have limited, shallow extent on one side of the fault compared to much greater vertical extent at depth on the other side of the fault (the thin-thick layers model of Grauch and Hudson, 2007). In these cases, the line is drawn along the narrowest HGM ridge, which represents the surface projection of the shallower of the two magnetic contrasts at the fault.

An interesting curved line interpreted as a fault ("contrast within Dry Union" on figs. 4 and 9) occurs in a fairly flat area in the northeastern part of the survey area, between the Arkansas River and Highway 285 (fig. 5). This curved line delineates a marked break in aeromagnetic pattern and some difference in magnetic values (fig. 2). The line is located entirely within an area mapped as thin (no more than 12 m (39 ft) thick) Quaternary fan alluvium (Scott and others, 1975). Further inspection of the geologic map suggests that basin-fill deposits of the Dry Union Formation directly underlie this fan alluvium on the northern and southern ends of the curved line and underlie 29 m (95 ft) of glacial outwash units at the Arkansas River. The preliminary depth estimates indicate the magnetic contrast

here is in the range of 50–150 m (164–492 ft) deep, which would put it within the Dry Union Formation. Moreover, at this depth, the marked difference in aeromagnetic pattern implies significant thickness of magnetic contrast. Thus, we interpret the magnetic source as a product of rift faulting. However, Rio Grande rift faults are typically steep normal faults, which would show much less curvature when projected to the surface. Perhaps this curved trace is associated with a fault splay in a complex area of faulting where strain is being transferred or is the cumulative effect of two crossing faults that were active at different times. Additional information from other geophysical data, magnetic modeling, and updated geologic mapping may elucidate the possibilities.

### East-West Anomaly North of Hot Springs

The western side of a prominent, east-west-elongated, ~200-nT aeromagnetic anomaly is located <1 km north of the hot springs and south of the town of Poncha Springs (crossed by profile A-A' on figs. 2 and 3). The anomaly is located in an area mapped as basin-fill sediments of the Dry Union Formation just north of a fault contact with Precambrian crystalline rocks (fig. 1; Van Alstine, 1975). The amplitude and width of the anomaly are much greater than would be expected from a magnetic contrast within the sediments, so the magnetic source is attributed to buried crystalline basement rocks. Profile A-A' across the eastern portion of this anomaly (fig. 11) shows its somewhat asymmetric shape, where the southern side of the anomaly has steeper slope than its northern side. The observed asymmetric profile can be fit to first order by a simple model of a tabular magnetic body, dipping about 70° to the north. The top edges of the modeled body underlie or parallel mapped faults in the Dry Union Formation (figs. 10 and 11). The model suggests that (1) basement is within 300 m (984 ft) of the surface as much as 1.5 km (0.9 mi) north of the contact between Dry Union Formation and Precambrian basement, and (2) intrabasement contacts in this area dip ~70° to the north and may be

controlled by or may themselves control rift-related faults. The proximity of this inferred intrabasement contact to the hot springs makes it an interesting target for ground-based exploration.

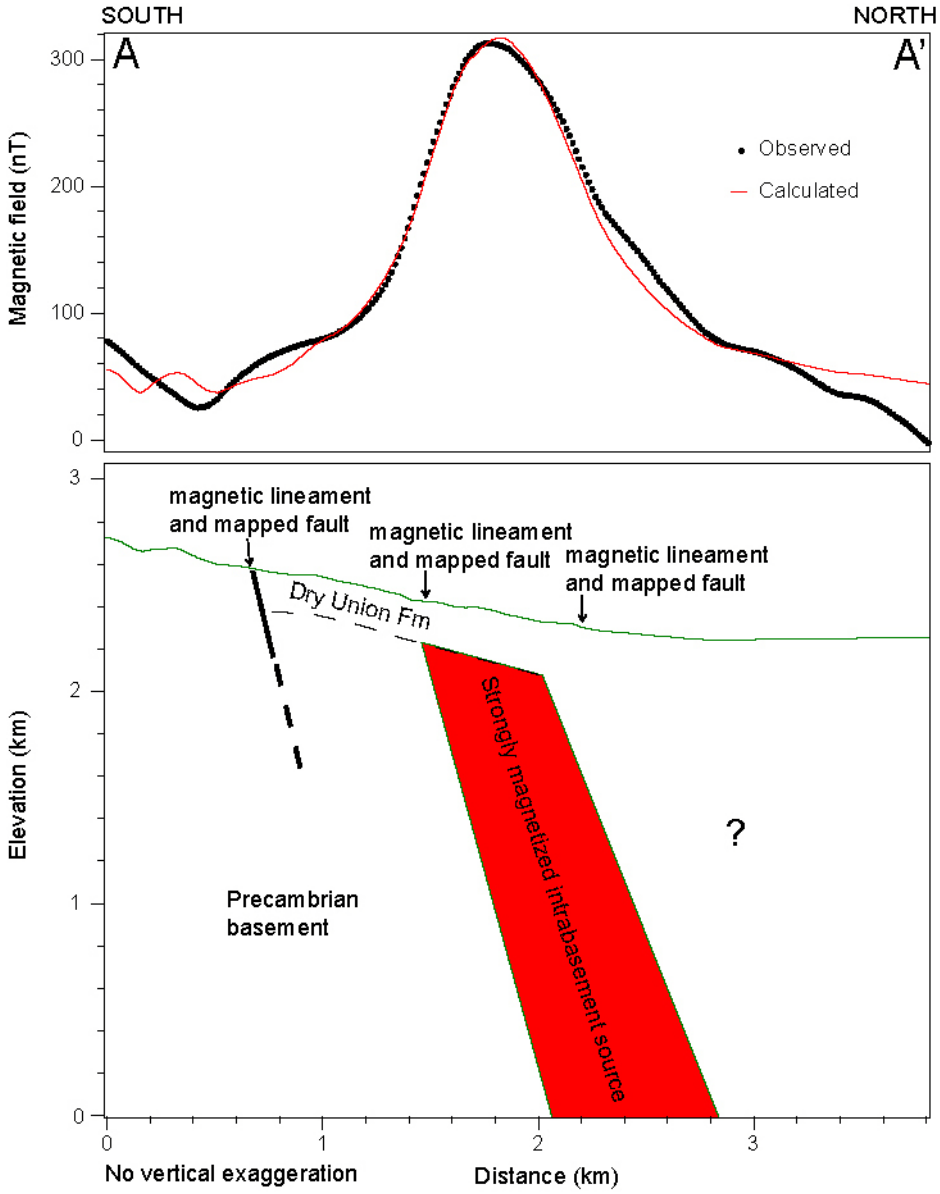


**Figure 11.** Profile and simple model along A-A'. RTP aeromagnetic data shown in upper panel and simple geologic model shown in lower panel. The tabular body (red) was assigned a magnetization of 1.4 A/m. Depth estimation techniques (program PDEPTH of Phillips, 1997) were used to locate the top edges of the body. Only the southern top edge is well constrained.

## Limitations

Although there are always errors in data acquisition and processing, by far the greatest limitations of the results come during the interpretation process, owing to assumptions relating magnetic properties of rocks to geologic units. Independent information, subjectivity, experience, or a combination of these is required. Below is a discussion of the limitations of the interpretations presented in this report.

The linear anomalies, where they are isolated from other magnetic sources and from manmade structures (such as pipelines or roads made of foreign materials), may be offset from the surface expression of faults for several reasons (Grauch and Hudson, 2007): (1) the magnetic contrast may be related to sedimentation near the fault rather than to offset material at the fault zone, (2) the fault may have shallow dip, (3) the fault at the surface may be a separate strand from the one at which the magnetic contrast occurs, or (4) the surface evidence of faulting has migrated away from the fault zone at depth because of erosion or subsequent sedimentation. Conversely, faults mapped at the surface may have no magnetic expression because (1) the units they offset have similar magnetic properties or (2) the amount of offset is minimal. In addition, even where faults are expressed magnetically, the sense of fault offset (which side is down) cannot be determined from the magnetic data alone.

Using horizontal gradients to enhance the locations of sources of the linear anomalies is useful, but interpretation of HGM can be ambiguous because of interference from neighboring sources, the presence of rugged topography, and the common, high variability of magnetic properties. For example, the locations of maxima of HGM can represent the locations of (1) faults, where a magnetic contrast is produced by structural juxtaposition of units, (2) contacts, where the magnetic contrast is produced by the limit of deposition of a magnetic unit against a less magnetic one such as the edge of volcanic flow, (3) steep topographic slopes, where the magnetic contrast is produced by the interface between rock and

air, or (4) abrupt changes in magnetization within one rock unit, produced by primary differences in magnetization or due to secondary destruction or growth of magnetic minerals. In addition, multiple gradients can occur where thin, horizontal, sheet-like sources are vertically offset from thicker sources at depth, represented by the thin-thick layers model of Grauch and Hudson (2007).

## Conclusions

High-resolution aeromagnetic data were acquired over the town of Poncha Springs and areas to the northwest to better map faults, especially where they are concealed. Understanding the fault patterns sheds light on potential pathways for migration of geothermal fluids such as those that discharge at the hot springs for which the town is named. The survey was an economical and efficient way to cover a large amount of ground, which was critical to gaining the detailed pattern of possible faulting in map view across the area.

Fault interpretation was accomplished by synthesizing interpretative maps derived from several different analytical methods, along with preliminary depth estimation (fig. 9). We generally followed different strategies within each of three different portions of the survey area, depending on the relation of aeromagnetic anomalies with topographic patterns. In the northwestern part of the area, aeromagnetic patterns have strong correspondence with west- to northwest-trending drainages incised in glacial outwash material. However, the aeromagnetic patterns contain more linear features and are straighter, suggesting an underlying structural control that requires field checking. Several west- to northwest-striking faults and one northeast-striking fault interpreted in this area are proposed mainly on the basis of differences in regional magnetic values.

In the mountainous terrain south of Highway 50, aeromagnetic patterns have much less correspondence with topographic patterns, suggesting that the majority of magnetic sources represent volumes of rocks that are mostly buried. Faults in this area were generally interpreted on the basis of

breaks in aeromagnetic patterns that follow linear trends. Interpreted faults in this area generally strike north-south or east-west, with northwest-striking faults near the hot springs. The interpreted faults are similar in strike and location to mapped faults (fig. 10).

In low-lying areas, many subtle linear features were interpreted as faults, many of which are concealed below the valley floor. Lineaments were not interpreted as faults where we judged them to be spurious or terrain-induced. Strikes are generally west-northwest near the mountain front south of Highway 50, east-northeast in the valley north of the town of Poncha Springs, and north in a swath about 3 km (~2 mi) west-northwest of the town. The western part of the west-northwest fault system may represent the Salida-Maysville fault inferred by Shannon and McAlpin (2006). The north-south zone of faults may be related to a buried, northward extension of the eastern margin of the southward projection of the rift basin (South Arkansas graben of Shannon and McAlpin, 2006) that extends south of the survey area (fig. 1). An interesting curved feature is located in a flat, low area between Highway 285 and the Arkansas River. We interpret this feature as a significant rift fault that offsets units within the underlying basin-fill sediments of the Dry Union Formation.

The interpreted and mapped faults together form a complementary dataset (fig. 10) that shows an overall pattern of criss-crossing fault zones, some of which step over where they cross. Estimates of depth to magnetic discontinuities indicate that nearly all magnetic sources associated with the possible faults are within 200 m (~660 ft) of the surface. In the sediment-covered areas, many of these faults offset the sediments at depths of 30–100 m (~100–330 ft); they may also extend deeper into the underlying bedrock. Numerous north-south-striking faults in the mountainous terrain south of highway 50 terminate on or near the west-northwest-striking zone of faults except ~3 km (2 mi) west-northwest the town of Poncha Springs, where there is a prominent juncture of west-northwest-, north-, and northwest-trending zones. This juncture is likely concealed just below the valley floor. From this

juncture, the more easterly striking zone of faults extends to the east, the west-northwest-striking zone of faults appears to step southward by about 1–2 km (0.6–1.25 mi) before continuing east to the vicinity of the hot springs, and the north-south zone of faults steps <1 km (<0.625 mi) to the west before extending farther to the north. The northwest-striking faults appear to extend from the vicinity of the hot springs on the southeast, through the area of the juncture, and align with the inferred fault to the northwest of the juncture.

The numerous fault intersections and complex fault patterns suggest a high density of faulting in the vicinity of Poncha Springs, both at the hot springs in the mountainous area 1.7 km (1.1 mi) south of town and hidden below valley fill ~3 km (~2 mi) west-northwest of town (fig. 10). Where basement rocks are involved in the faulting, the fracturing could enhance permeability that allows geothermal fluids to migrate or collect. The location of the hot springs at the intersection of a major northwest-striking interpreted fault and an east-striking mapped fault suggests that similar fault intersections elsewhere along the northwest-striking fault are prospective targets for follow-up investigation. Two such fault intersections are near the mountain front: one 1.5 km (0.9 mi) southwest of town and the other 1.9 km (1.2 mi) west of town. Because the fault patterns manifested by the aeromagnetic data in the valley originate from the sediments, follow-up investigations in these areas should evaluate whether shallow basement rocks are also involved in the faulting. Shallow basement is already indicated near the intersection 1.5 km (0.9 mi) southwest of town, which lies at the west end of an east-west elongated anomaly north of the hot springs. This anomaly likely originates from a magnetic portion of the Precambrian basement that is fairly shallow (<300 m or <984 ft), as indicated by a model over the east end of the anomaly.

The fault patterns revealed by the aeromagnetic data near Poncha Springs indicate a higher density of faulting than previously realized by geologic mapping alone. This high density may reflect

the location, which is at a structural transition between rift basins and shows evidence of thrusting and other structures related to the earlier Laramide orogeny (Shannon and McAlpin, 2006). The criss-crossing patterns are unusual in comparison to fault patterns observed in basins of the Rio Grande rift to the south, where faults observed from aeromagnetic data generally have northerly strikes (Grauch and Hudson, 2007). In these basins, multiple faults commonly curve toward each other and merge, but rarely do they cross one another obliquely. In another comparison, the geothermal reservoir at Dixie Valley, Nev. is generally located where multiple northwest-striking faults paralleling the range front merge with north-striking intrabasin faults, resulting in a high fault density in the vicinity of the reservoir (Smith and others, 2002). By analogy, the high fault density indicated for the Poncha Springs area provides many opportunities for follow-up geothermal investigations.

## Digital Files

Georegistered digital files included with this report are vector files representing the interpreted faults. The files are in shapefile format, a set of files with names that have the same prefix and suffixes of .prj, .shp, .shx, and .dbf. Visit the ESRI Web site (*http://www.esri.com*) for more information. Two sets of files are available: (1) faults interpreted with high confidence (prefix of psmagflts and psmagfltsNAD27) and (2) faults interpreted with less confidence (prefix of psmagflts_proposed and psmagflts_proposed NAD27). Projections are Universal Transverse Mercatur Projection, zone 13, with distances in meters. Files with "NAD27" in the prefix are projected using the North American Datum of 1927; the others are projected using the North American Datum of 1983.

## References Cited

Baranov, V., and Naudy, H., 1964, Numerical calculation of the formula of reduction to the magnetic pole: Geophysics, v. 29, p. 67–79.

Barret, J.K., and Pearl, R.H., 2006, An appraisal of Colorado's geothermal resources: Colorado Geological Survey Bulletin 39, CD-ROM.

Berkman, F.E., and Carroll, C.J., 2008, Interpretive heat flow map of Colorado: Colorado Geological Survey Map Series 45.

Blakely, R.J., 1995, Potential theory in gravity and magnetic applications: Cambridge University Press, 441 p.

Blakely, R.J., and Simpson, R.W., 1986, Approximating edges of source bodies from magnetic or gravity anomalies: Geophysics, v. 51, p. 1,494–1,498.

Case, J.E., and Sikora, R.F., 1984, Geologic interpretation of gravity and magnetic data in the Salida region, Colorado: U.S. Geological Survey Open-File Report 84–372, 46 p., 3 plates.

Cordell, L., and Grauch, V.J.S., 1985, Mapping basement magnetization zones from aeromagnetic data in the San Juan basin, New Mexico, *in* Hinze, W.J., ed., The utility of regional gravity and magnetic anomaly maps: Society of Exploration Geophysicists, p. 181–197.

Drenth, B.J., Grauch, V.J.S., Bankey, V., and New Sense Geophysics, Ltd., 2009, Digital data from the Great Sand Dunes and Poncha Springs aeromagnetic surveys, south-central Colorado: U.S. Geological Survey Open-File Report 2009-1089, *http://pubs.usgs.gov/of/2009/1089/.*

Duffield, W.A., and Sass, J.H., 2003, Geothermal energy—clean power from the Earth's heat: U.S. Geological Survey Circular 1249, 43 p.

Grauch, V.J.S., 2002, High-resolution aeromagnetic survey to image shallow faults, Dixie Valley geothermal field, Nevada: U.S. Geological Survey Open-File Report 02-384, 13 p.

Grauch, V.J.S., and Hudson, M.R., 2007, Guides to understanding the aeromagnetic expression of faults in sedimentary basins: Lessons learned from the central Rio Grande rift, New Mexico: Geosphere, v. 3, p. 596–623.

Grauch, V.J.S., Hudson, M.R., and Minor, S.A., 2001, Aeromagnetic expression of faults that offset basin fill, Albuquerque basin, New Mexico: Geophysics, v. 66, p. 707–720.

Grauch, V.J.S., and Johnston, C.S., 2002, Gradient window method—A simple way to separate regional from local horizontal gradients in gridded potential-field data: 2002 Society of Exploration Geophysicists Technical Program Expanded Abstracts, 72nd Annual Meeting, v. 21, p. 762–765.

Hansen, R.O., Racic, L., and Grauch, V.J.S., 2005, Magnetic methods in near-surface geophysics, *in* Butler, D.K., ed., Near-surface geophysics: Society of Exploration Geophysicists Investigations in Geophysics No. 13: Tulsa, Okla., Society of Exploration Geophysicists, p. 151–175.

Hudson, M.R., Grauch, V.J.S., and Minor, S.A., 2008, Rock magnetic characterization of faulted sediments with associated magnetic anomalies in the Albuquerque basin, Rio Grande rift, New Mexico: Geological Society of America Bulletin, v. 120, p. 641–658.

Phillips, J.D., 1997, Potential-field geophysical software for the PC, version 2.2: U.S. Geological Survey Open-File Report 97-725.

Phillips, J.D., 2000, Locating magnetic contacts—A comparison of the horizontal gradient, analytic signal, and local wavenumber methods: 2000 Society of Exploration Geophysicists Technical Program Expanded Abstracts, 70th Annual Meeting, v. 19, p. 402–405.

Phillips, J.D., Hansen, R.O., and Blakely, R.J., 2007, The use of curvature in potential-field interpretation: Exploration Geophysics, v. 38, p. 111–119.

Reid, A.B., 1980, Aeromagnetic survey design: Geophysics, v. 45, p. 973–976.

Reynolds, R.L., Rosenbaum, J.G., Hudson, M.R., and Fishman, N.S., 1990, Rock magnetism, the distribution of magnetic minerals in the Earth's crust, and aeromagnetic anomalies: U. S. Geological Survey Bulletin 1924, p. 24–45.

Scott, G.R., Van Alstine, R.E., and Sharp, W.N., 1975, Geologic map of the Poncha Springs Quadrangle, Chaffee County, Colorado: U.S. Geological Miscellaneous Field Studies Map no. 658, 1:62,500 scale map.

Shannon, J.R., and McCalpin, J.P., 2006, Geologic map of the Maysville Quadrangle, Chaffee County, Colorado: Colorado Geological Survey Open-File Report 06-10, 1:24,000 scale map.

Smith, R.P., Grauch, V.J.S., and Blackwell, D.D., 2002, Preliminary results of a high-resolution aeromagnetic survey to identify buried faults at Dixie Valley, Nevada: Geothermal Resources Council Transactions, v. 26, p. 543–546.

Smith, R.S., Thurston, J.B., Dai, T.-F., and MacLeod, I.N., 1998, iSPI™—The improved source parameter imaging method Geophysical Prospecting, v. 46, p. 141–151.

Thurston, J.B., and Smith, R.S., 1997, Automatic conversion of magnetic data to depth, dip, and susceptibility contrast using the SPI method: Geophysics, v. 62, p. 807–813.

Tweto, O., 1979, Geologic map Of Colorado: U.S. Geological Survey, 1:500,000 scale map.

Van Alstine, R.E., 1975, Geologic map of the Bonanza NE Quadrangle, Chaffee and Saguache Counties, Colorado: U.S. Geological Survey Open-File Report 75-53, 1:62,500 scale map.